UC Santa Cruz

UC Santa Cruz Previously Published Works

Title

A Slow Conformational Switch in the BMAL1 Transactivation Domain Modulates Circadian Rhythms

Permalink

https://escholarship.org/uc/item/9c42d068

Journal

Molecular Cell, 66(4)

ISSN

1097-2765

Authors

Gustafson, Chelsea L
Parsley, Nicole C
Asimgil, Hande
et al.

Publication Date

2017-05-01

DOI

10.1016/j.molcel.2017.04.011

Peer reviewed

eScholarship.org Powered by the California Digital Library
University of California

Author Manuscript

Author Manuscript

Author Manuscript

Author Manuscript

HHS Public Access

Author manuscript

Mol Cell. Author manuscript; available in PMC 2018 May 18.

Published in final edited form as:

Mol Cell. 2017 May 18; 66(4): 447–457.e7. doi:10.1016/j.molcel.2017.04.011.

A slow conformational switch in the BMAL1 transactivation domain modulates circadian rhythms

Chelsea L. Gustafson[1,6], **Nicole C. Parsley**[1], **Hande Asimgil**[1], **Hsiau-Wei Lee**[1], **Christopher Ahlbach**[1], **Alicia K. Michael**[1], **Haiyan Xu**[2], **Owen L. Williams**[1], **Tara L. Davis**[3], **Andrew C. Liu**[2,4], and **Carrie L. Partch**[1,5,*]

[1]Department of Chemistry and Biochemistry, University of California Santa Cruz, Santa Cruz, CA, 95064 USA

[2]Department of Biological Sciences, University of Memphis, Memphis, TN, 38152 USA

[3]Drexel University College of Medicine, Philadelphia, PA, 19104 USA

[4]Feinstone Genome Research Center, University of Memphis, Memphis, TN, 38152 USA

[5]Center for Circadian Biology, University of California San Diego, San Diego, CA, 92093 USA

SUMMARY

The C-terminal transactivation domain (TAD) of BMAL1 (Brain and muscle ARNT-like 1) is a regulatory hub for transcriptional coactivators and repressors that compete for binding and consequently contributes to period determination of the mammalian circadian clock. Here, we report the discovery of two distinct conformational states that slowly exchange within the dynamic TAD to control timing. This binary switch results from *cis/trans* isomerization about a highly conserved Trp-Pro imide bond in a region of the TAD that is required for normal circadian timekeeping. Both *cis* and *trans* isomers interact with transcriptional regulators, suggesting that isomerization could serve a role in assembling regulatory complexes *in vivo*. Towards this end, we show that locking the switch into the *trans* isomer leads to shortened circadian periods. Furthermore, isomerization is regulated by the cyclophilin family of peptidyl-prolyl isomerases, highlighting the potential for regulation of BMAL1 protein dynamics in period determination.

TOC Image

*Corresponding author: Carrie L. Partch, cpartch@ucsc.edu, Telephone: 831-459-3905, University of California Santa Cruz, 1156 High St. Mailstop: Chemistry, Santa Cruz, CA 95064.

[6]Present address: Department of Natural Sciences, Oregon Institute of Technology, Wilsonville, OR 97070 USA

Lead contact: Carrie L. Partch

Publisher's Disclaimer: This is a PDF file of an unedited manuscript that has been accepted for publication. As a service to our customers we are providing this early version of the manuscript. The manuscript will undergo copyediting, typesetting, and review of the resulting proof before it is published in its final citable form. Please note that during the production process errors may be discovered which could affect the content, and all legal disclaimers that apply to the journal pertain.

Author Contributions

C.L.G., N.C.P., H.A., H.W.L. and C.L.P. designed the experiments. C.L.G., N.C.P., H.A., C.A., A.K.M. and C.L.P. collected data. H.X., O.L.W. and T.L.D. contributed reagents or analytical tools. A.C.L. and C.L.P. supervised the experiments. C.L.G. and C.L.P. wrote the manuscript with contributions from T.L.D. and A.C.L. All authors reviewed the manuscript and approve of the conclusions.

Author Manuscript Author Manuscript Author Manuscript Author Manuscript

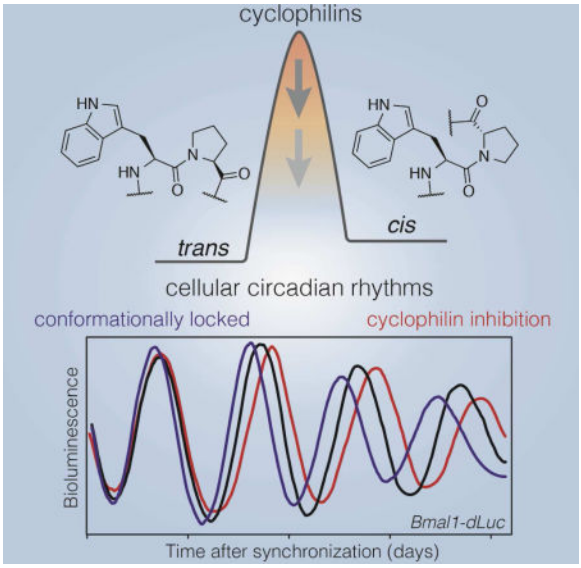

Keywords

circadian rhythms; NMR spectroscopy; transcriptional activation; proline isomerization; cyclophilins; cyclosporin A

Mammalian circadian clocks are intrinsic molecular timekeeping systems that coordinate physiological processes with external environmental cues in order to appropriately time daily activities. This coordination is achieved by two interlocked transcription feedback loops that control the temporal basis of expression for over 40% of the mammalian genome (Zhang et al., 2014). The heterodimeric transcription factor CLOCK:BMAL1 sits at the core of the primary feedback loop that directs the chronometric transcription of clock-controlled genes. Circadian timekeeping is established through the coordinate regulation of CLOCK:BMAL1 by transcriptional coactivators, such as CBP/p300, and the dedicated circadian repressors PER and CRY (Partch et al., 2014). Many processes contribute to the timing of activation and repression, such as the localization, phosphorylation, and degradation of repressors in the nucleus (reviewed in (Gallego and Virshup, 2007)). However, the mechanisms that regulate the changing architecture of CLOCK:BMAL1 transcriptional regulatory complexes throughout the day are still poorly understood (Koike et al., 2012). The highly dynamic BMAL1 transactivation domain (TAD) is one hub for these interactions, as it interacts with both coactivators and repressors and is necessary for circadian oscillations (Kiyohara et al., 2006; Park et al., 2015; Xu et al., 2015). Modulating affinity of the BMAL1 TAD for its regulators elicits large changes in period, demonstrating an important role in timekeeping of the transcription-based clock (Xu et al., 2015). Identification of processes that fine-tune interactions between the BMAL1 TAD and transcriptional regulators will shed light on the mechanism by which animals measure time and use it to coordinate behavior and physiology with the environment.

By inducing changes in conformation, protein-protein interactions, or subcellular localization, post-translational modifications play critical roles in controlling signaling

Author Manuscript Author Manuscript Author Manuscript Author Manuscript

pathways and information processing. Additionally, proteins exhibit a range of dynamic behaviors on different timescales that can also contribute to functional output (Henzler-Wildman and Kern, 2007). From the fast, stochastic motions of intrinsically disordered regions to the longer timescales of coordinated domain motions and protein folding, the dynamic behavior of proteins ultimately governs how they regulate biological processes. One such behavior is conformational *cis/trans* isomerization about a proline-containing imide peptide bond (Xaa-Pro); popularly dubbed a *molecular timer* (Lu et al., 2007), isomerization is an intrinsically slow process (milliseconds to minutes) that can be enzymatically accelerated by peptidyl prolyl isomerases (PPIases) by up to ~4–5 orders of magnitude (Schmid, 1993). Proline isomerization is relatively rare, as only ~6% of imide bonds are estimated to undergo isomerization (Stewart et al., 1990), but it has a profound impact on diverse cellular processes, such as transcription (Bataille et al., 2012; Nelson et al., 2006), protein folding (Wedemeyer et al., 2002), ion channel gating (Lummis et al., 2005), and protein degradation (Liou et al., 2011). Likewise, proline isomerases are pivotal components of many intracellular signaling pathways through their acceleration of this otherwise slow process (Brazin et al., 2002; Lang et al., 1987; Saleh et al., 2016). Dysfunctional regulation of proline isomerization and/or PPIase activity has been implicated in cancer (Zhou and Lu, 2016), Alzheimer's disease (Nakamura et al., 2012) and regulation of circadian rhythms in *Drosophila* (Kang et al., 2015).

Here, we report the discovery of a slow conformational switch in the BMAL1 TAD that modulates mammalian circadian rhythms. Using NMR spectroscopy, we show that *cis/trans* isomerization about a conserved Trp-Pro imide bond generates this conformational exchange, which we have dubbed the 'TAD switch'. To study the roles of individual isomers in interactions with circadian transcriptional regulators, we developed locked *cis* and *trans* isomers using site-directed mutagenesis or peptide synthesis with unnatural amino acids. Locked isomers bind CRY1 and CBP KIX with similar affinities, yet locking the TAD into its *trans* isomer shortens the circadian period in cell-based assays, demonstrating that exchange between these two conformations contributes to circadian timekeeping. Using NMR, we determined that the timescale of isomerization is intrinsically slow, taking minutes to complete a cycle of exchange. We then identified a group of PPIases within the cyclophilin family that significantly enhance rates of isomerization. Inhibition of cyclophilins lengthens circadian period in a switch-dependent manner, suggesting that enzymatic modulation of intrinsically slow dynamics at the BMAL1 TAD could play a role in tuning the circadian period *in vivo*.

RESULTS

PROLINE ISOMERIZATION ACTS AS A MOLECULAR SWITCH IN THE C-TERMINUS OF BMAL1

The BMAL1 TAD acts as a regulatory hub that interacts with positive or negative transcriptional regulators as a function of circadian time (CT) to control the activation state of CLOCK:BMAL1 (Koike et al., 2012). We previously used NMR spectroscopy to identify overlapping binding sites of the transcriptional coactivator CBP/p300 and the repressor CRY that map to two distinct sites in the BMAL1 TAD: the predicted alpha helical region in the

Author Manuscript Author Manuscript Author Manuscript Author Manuscript

center of the TAD and the extreme C-terminus (Figure 1A) (Xu et al., 2015). ^{15}N-^{1}H heteronuclear single quantum coherence (HSQC) NMR spectra display a peak for each of the constituent N-H bonds in the disordered TAD. The chemical shift, or location of the peaks, represents a population-weighted average of conformations that interconvert in fast exchange. To our surprise, the ^{15}N-^{1}H HSQC spectrum of the BMAL1 TAD revealed two distinct resonances for each of the 8 C-terminal residues (Figures 1B and S1A), indicating slow exchange between two conformations localized to this distal site. We performed liquid chromatography/mass spectrometry analysis on the ^{15}N-labeled NMR sample, which demonstrated the presence of a single, highly pure peptide of the expected molecular weight (Figures S1B–C). Moreover, truncation of the C-terminal 7 residues resulted in a ^{15}N-^{1}H HSQC spectrum devoid of peak doubling, confirming that chemical exchange requires the extreme C-terminus of the TAD (Figure S1A).

To identify the structural basis for this conformational heterogeneity, we turned to the C(CO)NH TOCSY NMR experiment, which correlates sidechain carbon chemical shifts with the following amide peptide bond to provide sequence-specific information about the local environment. Looking back from the doubled amide peaks for residue L626, the chemical shifts of P625 $^{13}C_{\beta}$ and $^{13}C_{\gamma}$ atoms unambiguously identified that the W624–P625 imide bond is found in two distinct conformations, a *cis* and a *trans* form based on a comparison to NMR chemical shift databases (Figures 1C, D) (Shen and Bax, 2010). No *cis* isomer was detected for P623 or any of the other three imide bonds in the BMAL1 TAD construct (Figures 1C and S1D–F), demonstrating that peak doubling in the C-terminus is due solely to slow isomerization of the Trp-Pro bond. Using the relative abundance of several representative peaks of the two isomers, we determined that the population of the TAD switch under these conditions is approximately 65% *trans* and 35% *cis* isomers (Figure S1G).

CONSERVATION OF THE TAD SWITCH FROM INSECTS TO VERTEBRATES

To begin exploring the functional significance of the TAD switch, we first examined its conservation across BMAL orthologs (Figure 1E). We noted that the proline of the switch is not conserved in vertebrate BMAL2, a homolog of BMAL1 that has an active TAD but cannot sustain circadian cycling outside of the suprachiasmatic nucleus (Shi et al., 2010; Xu et al., 2015). Phylogenetic analysis of CYCLE, the insect ortholog of BMAL1, demonstrates its divergence into two distinct gene families: a *Drosophila*-like CYCLE (dCYC) that possesses only the N-terminal bHLH, PAS-A, and PAS-B domains, and a vertebrate BMAL1-like CYCLE that also contains the C-terminal TAD (Chang et al., 2003). The BMAL1-like CYCLE genes found in insects also possess a vertebrate-like cryptochrome with transcriptional repressor activity, suggesting that the network architecture of these molecular clocks is similar to vertebrates (Rubin et al., 2006; Zhu et al., 2008). Because these insect CYC genes exhibit higher functional and structural homology to vertebrate BMAL1 than *Drosophila* CYC, we hereafter refer to these genes as insect-BMAL1 (iBMAL1). We found that the TAD switch is strictly conserved in all iBMAL1 genes, indicating that the presence of the switch in BMAL1 predates the divergence of insects and vertebrates about 600 million years ago (Peterson et al., 2004).

Author Manuscript Author Manuscript Author Manuscript Author Manuscript

Although the eight residues of the BMAL1 TAD switch are highly conserved throughout metazoans, we noted several substitutions upstream of the conserved Trp-Pro switch and the inclusion of an additional C-terminal proline in some invertebrates (Figure 1E). To determine if these sequence variations affect the switch, we synthesized 8-mer peptides using the vertebrate BMAL1 and *Apis florea* iBMAL1 sequences and analyzed peak intensities from ^{15}N-^{1}H HSQC spectra collected on natural abundance samples. The vertebrate switch peptide (FSDLPWPL) displayed an equilibrium population of isomers similar to the intact mouse BMAL1 TAD (Figures 1F and S1G–H), as did the iBMAL1 switch peptide (FSGLPWPLP) (Figure 1F), suggesting that insects with a vertebrate-like clock likely share switch functionality with mouse BMAL1.

TRP AND PRO ARE THE KEY RESIDUES COMPRISING THE TAD SWITCH

To probe the importance of the two switch isomers on circadian rhythms, we first set out to identify local sequence requirements that contribute to the TAD switch. By carefully defining these local factors *in vitro*, we aimed to validate a set of molecular tools that would allow us to explore switch function in the cellular environment. With rare exception, only proline allows the *cis* isomer to arise in a peptide bond (Pal and Chakrabarti, 1999). As expected, mutation of P625 to Ala eliminated detection of the *cis* isomer by NMR, providing us with a *trans*-locked BMAL1 (Figures 2A, B). Conversely, integration of the bulky analog 5,5-dimethyl Proline (dmP) (Lummis et al., 2005; Nakamura et al., 2012) in place of P625 produced the opposite effect, a TAD switch exclusively populating the *cis* isomer (Figures 2A, B). The backbone geometry of these mutants was verified using ^{13}C-^{1}H HSQC and ^{1}H-^{1}H TOCSY spectra collected on natural abundance peptides (Figures S2A, B). The P625A *trans*-locked switch mutant was also incorporated into the intact BMAL1 TAD (residues 579–626) to establish that *cis*/*trans* isomer ratios were similar by NMR spectroscopy (Figure S2C).

Long range interactions affecting the equilibrium population of *cis*/*trans* isomers have been reported in some highly structured systems (Wedemeyer et al., 2002), but for intrinsically disordered regions such as the BMAL1 TAD, long range constraints are unlikely to affect isomerization (Theillet et al., 2014). By contrast, the identity of the (*i-1*) residue that precedes the proline has a profound impact on the equilibrium population of *cis* isomers. Aromatic amino acids in the (*i-1*) position increase the propensity of an imide bond to sample the *cis* conformation through stabilizing interactions of the π aromatic face with the proline C–H_α bond (Zondlo, 2013), while small electron-poor amino acids typically decrease stability of the *cis* isomer (Reimer et al., 1998; Shen and Bax, 2010). As predicted, the replacement of W624 with Ala resulted in no observable *cis* isomer population in both the 8-mer peptide and the intact TAD (Figures 2A, B and S2A–C). Likewise, decreasing the aromaticity of the (*i-1*) residue by substitution of W624 to Tyr resulted in a decrease in the *cis* population (Figures 2A and S2A, B). Altogether, these data demonstrate that both Trp and Pro residues are important for the observed conformational switch in the BMAL1 TAD.

THE *TRANS*-LOCKED TAD SWITCH DRIVES SHORTENED CIRCADIAN RHYTHMS

Mutations in the BMAL1 TAD elicit control over the period of the transcription-based clock by differentially regulating affinity for transcriptional coactivators and repressors. For

Author Manuscript Author Manuscript Author Manuscript Author Manuscript

example, substitution of two key residues in the central alpha helical region of the TAD (L606A/L607A) disrupted circadian rhythms altogether by eliminating interactions with regulators, while other mutations led to circadian periods from ~19 to 26 hours; notably, deletion of the last 7 residues of the TAD (619X, referred to as Δswitch here) shortened the intrinsic period by approximately 3 hours (Xu et al., 2015). To examine the functional consequences of disrupting the TAD switch on circadian rhythms, we stably incorporated different *trans*-locked *Bmal1* mutants into *Bmal1*$^{-/-}$;*Per2*^{Luc} cells. In our hands, complementation with wild type *Bmal1* resulted in a period of approximately 23 hours (Figures 2C, D and S2D–E), while the P625A mutant decreased this period by over 1 hour. Complementation with W624A *Bmal1* led to a ~3 hour decrease in period, on par with the shortened period observed upon deletion of the entire switch region (Figures 2C, D and S2D–E) (Xu et al., 2015). Moreover, the W624A/P625A double mutant exhibited a short period similar to the W624A mutant (Figure S2D–E), demonstrating that while locking the switch into the *trans* isomer has a significant effect on period, this effect is further enhanced by deletion of the bulky aromatic sidechain of W624.

BOTH ISOMERS OF THE TAD SWITCH INTERACT WITH TRANSCRIPTIONAL REGULTORS

To begin to probe the molecular mechanism for the short period phenotype observed upon complementation with *trans*-locked mutants of *Bmal1*, we quantitatively analyzed the interaction of *cis* and *trans* isomers of the TAD with known transcriptional regulators using NMR and fluorescence anisotropy. NMR studies performed on the wild-type ^{15}N BMAL1 TAD demonstrated that the CC helix and KIX domains of regulators CRY1 and CBP, respectively, each interact with both isomers present in the native TAD (Figure 3A, left panels). The same ^{15}N-^{1}H HSQC titration experiment was also performed on the *trans*-locked ^{15}N BMAL1 TAD P625A mutant, giving rise to chemical shift changes that were highly similar to those of the native *trans* isomer (Figures 3A, right panels, and Figure S3A–C), suggesting that the P625A mutant is a reasonable proxy for the native *trans* isomer of the TAD.

We then determined affinities of locked variants of the TAD switch for CRY1 and the CBP KIX domain using fluorescence anisotropy with short labeled BMAL1 TAD peptides encompassing the highly conserved region from residues 594–626 (Xu et al., 2015). To promote robust changes in fluorescence polarization from the short TADs, we elected to use the ~50kDa CRY1 photolyase homology region (PHR) that contains the CC helix instead of the isolated CC peptide because they have similar affinity for the TAD (Czarna et al., 2013; Xu et al., 2015). In this assay, both WT and Δswitch TADs bound the CRY1 PHR and CBP KIX domain with affinities similar to those previously determined by isothermal titration calorimetry (Figure 3B and Table 1) (Czarna et al., 2013; Xu et al., 2015). Moreover, analysis of the CRY1 binding curve suggested positive cooperativity with a Hill coefficient of 1.6, possibly arising from enforced proximity effects (Ferrell and Cimprich, 2003; Pullen and Bolon, 2011) of the two CRY1 binding motifs at the central alpha helix and switch region of the TAD. In support of this, truncation of the switch region eliminated the apparent cooperativity (Table 1), further demonstrating its importance for interactions with regulators. However, binding assays with *cis* and *trans*-locked short TADs demonstrated that affinities for the CRY1 PHR and CBP KIX domain were similar to wild-type (Figure 3B, Table 1 and

Author Manuscript Author Manuscript Author Manuscript Author Manuscript

Figure S3D–E), indicating that effects of the TAD switch on circadian period appear not to arise from differential affinity for either of the known binding partners under these conditions.

ISOMERIZATION OF THE TAD SWITCH OCCURS ON THE TIMESCALE OF MINUTES

The ability to switch between distinct protein conformations can regulate signaling by modulating affinity or occluding binding interfaces (Brazin et al., 2002; Sarkar et al., 2007), or by exerting kinetic control over isoenergetic conformational states to influence the selection of partners (Phillips et al., 2013). Isomerization about the imide bond is an inherently slow process, leading to experimentally determined rates of proline isomerization from milliseconds to nearly an hour *in vitro* (Eckert et al., 2005; Grathwohl and Wuthrich, 1981), considerably longer than the nanosecond backbone dynamics typically encountered in disordered proteins (Henzler-Wildman and Kern, 2007). To determine the timescale of exchange between *cis* and *trans* isomers in the BMAL1 TAD, we used ^{15}N-^{1}H ZZ exchange NMR experiments that incorporate a short delay after encoding the ^{15}N frequency to capture interconversion via formation of cross peaks that align with the ^{1}H frequency of the new state. When performed at 25°C, the absence of characteristic cross peaks in the ^{15}N-^{1}H ZZ exchange assay (Figure 4A) demonstrated that isomerization was too slow to be detected at room temperature. Because intrinsically disordered proteins like the BMAL1 TAD already lack structural elements that are typically disrupted by high temperature, we increased the temperature to enhance isomerization rates. First, we collected a series of ^{15}N-^{1}H HSQC spectra at increasing temperatures up to 70°C (Figures 4B and S4A), observing that integrity of the BMAL1 TAD was retained after incubation at temperatures up to 70°C, with an essentially identical ^{15}N-^{1}H HSQC spectrum upon return to 25°C (Figure S4B), indicating no lasting effect of high temperature on the protein.

To explore the effect of temperature on switch kinetics, we collected ^{15}N-^{1}H ZZ exchange datasets at increasing temperatures until we observed cross peaks indicative of exchange. These cross peaks first appeared at 55°C and grew in intensity with increasing temperature (Figure 4C). Intensities for peaks representing *cis* and *trans* isomers of the W624 side chain indole and L626 backbone amide, as well as exchange cross peaks, were extracted and plotted as a function of delay time (Figure S4C). Exchange rates were calculated independently for temperatures from 55–65°C using the Bloch-McConnell equations (Farrow et al., 1994). We then plotted temperature-dependent exchange rates using the Eyring equation to extrapolate the kinetics of exchange to temperatures lower than 55°C (Figure 4C and Supplemental Table 1). At 25°C, the time for *cis* to *trans* isomerization is calculated to take 3.64 minutes, while *trans* to *cis* isomerization takes 6.30 minutes, for an overall exchange lifetime of approximately 10 minutes. Based upon these data, we calculated a barrier for *cis*/*trans* isomerization of ~20.4 kcal/mol, with a difference in stability between the two isomers of ~0.5 kcal/mol (Figure 4D), both on par with values for analogous systems (Reimer et al., 1998). Compared to the fast motions of the intrinsically disordered TAD backbone suggested by predominantly negative heteronuclear ^{15}N-^{1}H NOE values (Figure S4D), slow isomerization of the Trp-Pro imide bond suggests that functionally relevant conformational dynamics may exist over at least twelve orders of magnitude in timescale in the BMAL1 TAD (Figure S4E).

Author Manuscript Author Manuscript Author Manuscript Author Manuscript

CYCLOPHILINS CAN ACCELERATE INTERCONVERSION OF THE TAD SWITCH

Intrinsically slow rates of *cis/trans* isomerization are often enhanced catalytically by peptidyl-prolyl isomerases to regulate cellular signaling events. Notably, peptidyl-prolyl isomerases regulate circadian rhythms in *Drosophila*; however, activity of the Pin1-like Dodo isomerase is phosphoserine-specific and appears to target PER proteins (Kang et al., 2015). Given that the BMAL1 TAD doesn't possess this phosphospecific consensus motif, we chose to focus our initial attention on cyclophilins for two reasons. First, the broadly expressed peptidyl prolyl isomerase A (PPIA; also known as Cyclophilin A, CypA) co-immunoprecipitated with BMAL1 in a screen for interacting partners (Lipton et al., 2015), and second, the cyclophilin family has eight isoforms with nuclear localization (Adams et al., 2015) where we believe regulation of the TAD is likely to occur. To determine if PPIA could regulate the TAD switch *in vitro*, we performed a ^{15}N-^{1}H ZZ exchange NMR experiment on the BMAL1 TAD at room temperature in the presence of sub-stoichiometric concentrations of PPIA. As cyclophilins have notoriously low K_ms (0.3–1 mM) for their substrates (Coelmont et al., 2010; Schmid, 1993) this precluded a traditional analysis of the catalytic efficiency of PPIA for the TAD. However, we found that PPIA increased the relative rate of isomerization at room temperature by ~300-fold (Figure 5A).

We subsequently purified and assayed each of the predominantly nuclear cyclophilins PPIE, PPIG, PPIH, PPIL1, PPIL2, PPIL3, PPWD and CWC27 for activity against the TAD switch by acquiring ^{15}N-^{1}H ZZ exchange data under similar conditions at room temperature. We found that the cyclophilins PPIE, PPIG, PPIH, PPIL1, PPIL3 all significantly increased the rate of isomerization in BMAL1, although their acceleration of exchange rates in the TAD varied by over 10-fold (Figures 5A, B). By contrast, the isomerases PPIL2, PPWD, and CWC27 were either not active on the TAD or had activity that was below the detection limit of our ^{15}N-^{1}H ZZ exchange assay. Both PPIL2 and CWC27 were previously shown to lack activity on generic peptide substrates used to assay cyclophilin activity, suggesting they are catalytically dead (Davis et al., 2010). We then explored if cyclophilin activity on the TAD was restricted to isoforms with nuclear localization by testing the activity of PPIF (also known as CypD), which is localized exclusively in mitochondria (Lin and Lechleiter, 2002). We found that PPIF was at least as active on the TAD as the top-ranked nuclear cyclophilins in our assay (Figures 5A, B), indicating that cyclophilins can exhibit robust activity on the BMAL1 TAD when removed from a cellular context that might otherwise impart substrate selectivity. To date, very little is known about factors that dictate the substrate selectivity or activity of cyclophilins, although they share relatively similar active sites (Davis et al., 2010). Notably, some of the cyclophilins that are active on the BMAL1 TAD *in vitro* are also expressed in a circadian manner *in vivo* (Figure S5, (Pizarro et al., 2013)). Therefore, the selectivity and/or activity of cyclophilins on the TAD may be conferred *in vivo* by regulated changes in abundance, subcellular localization or through formation of different regulatory complexes with CLOCK:BMAL1 throughout the day (Koike et al., 2012; Lee et al., 2001).

INHIBITION OF CYCLOPHILINS INCREASES CIRCADIAN PERIOD LENGTH

To explore if cyclophilins influence timekeeping by the mammalian circadian clock, we treated human U2OS osteosarcoma cells stably transfected with a *Bmal1-dLuc* bioluminescent circadian reporter (Vollmers et al., 2008) with the broad specificity

Author Manuscript Author Manuscript Author Manuscript Author Manuscript

cyclophilin inhibitor, Cyclosporin A (CsA). This cell permeable cyclic peptide binds to the active site of the cyclophilin family with affinities ranging from ~5–500 nM (Davis et al., 2010). We observed dose-dependent lengthening of circadian period with low doses of CsA (Figures 5C, D), while at high concentrations (>15 μM), it induced arrhythmicity (data not shown). To probe the selectivity of CsA on cyclophilin regulation of the BMAL1 TAD, we performed two additional orthogonal assays. First, we examined whether the long period phenotype could be attributed to inhibition of the phosphatase PP2B, as CsA can also direct the assembly of inhibitory ternary complexes of cyclophilins with PP2B (Huai et al., 2002; Liu et al., 1991). The effect of CsA on circadian period appeared to be independent of PP2B, as we found that treatment with Deltamethrin, a cyclophilin-independent PP2B inhibitor (Enan and Matsumura, 1992) did not elicit a change in period (Figures 5C, D). Therefore, broad inhibition of isomerase activity in the cyclophilin family leads changes in circadian period.

We then wanted to determine the degree to which CsA-dependent changes in period arose from regulation of the BMAL1 TAD switch. To do this, we utilized stable *Bmal1*$^{-/-}$;*Per2*^{Luc} cell lines complemented with either wild-type *Bmal1* or two *trans*-locked *Bmal1* mutants, P625A or the W624A/P625A (Figure 2 and S5). We reasoned that any CsA-dependent period changes in the mutant lines could not be due to regulation of the switch by cyclophilins, as the *cis* isomer of the switch was eliminated upon introduction of these mutations (Figures 2 and S2). Consistent with this model, we observed a significant decrease in period lengthening by CsA in both *trans*-locked cell lines compared to cells complemented with wild-type *Bmal1* (Figure 5E and S5). Switch-independent changes in period, particularly at the highest concentration of CsA tested (10 μM), demonstrate that regulation of other pathways aside from the TAD switch by cyclophilins can also influence circadian timing. Taken together, our data support a role for an intrinsically slow conformational switch in the BMAL1 TAD in regulation of circadian period and lay the foundation for studies of clock regulation by cyclophilins, a broadly expressed, yet poorly studied, class of enzymes.

DISCUSSION

Here we present our discovery of a slow conformational switch in the BMAL1 TAD that participates in regulation of timekeeping by the mammalian circadian clock. Using NMR spectroscopy, we identified that *cis/trans* isomerization about the W624-P625 imide bond at the C-terminus of BMAL1 underlies the molecular basis for this binary switch. Consistent with previous studies on the composition and rarity of other switches based on *cis*/*trans* isomerization (Shen and Bax, 2010; Stewart et al., 1990), we found that both proline and tryptophan side chains make critical contributions to the relatively high *cis* population observed in the BMAL1 TAD. These two residues are conserved from humans to invertebrates (including insects other than *Drosophila*) that have a vertebrate-like clock architecture (Chang et al., 2003), suggesting an ancient role for the TAD switch in regulation of CLOCK:BMAL1 activity. We used mutation of the Trp and Pro sites to generate a suite of TAD proteins with varying *cis*/*trans* populations or mutants that were altogether ‘locked’ into discrete *cis* or *trans* isomers. By coupling cell-based studies of circadian oscillations with solution biophysical techniques that probed structural and biochemical constraints of

Author Manuscript Author Manuscript Author Manuscript Author Manuscript

the TAD switch, we were able to demonstrate that perturbing switch function alters circadian timing. Moreover, we identified that cyclophilins can accelerate interconversion *in vitro* and influence circadian timing in clock cells in a switch-dependent manner, suggesting that cyclophilins regulate the clock at least partly through control of the TAD switch.

There is growing evidence that the flexible BMAL1 TAD plays an important role in control of circadian timekeeping. Given that transcription-based feedback loops establish the mammalian circadian clock, factors that influence how the CLOCK:BMAL1 interacts with regulators are likely to play a key role in timekeeping (Gustafson and Partch, 2015). The conformational switch we identified by NMR is located in the C-terminus of an intrinsically disordered transactivation domain that is essential for CLOCK:BMAL1 activity and circadian timekeeping (Park et al., 2015; Xu et al., 2015). Notably, the importance of this switch region was first highlighted a decade ago in a transposon-based screen to identify functionally important regions of BMAL1; Yagita and colleagues noted that truncation of the last 7 amino acids of BMAL1 decreased CLOCK:BMAL1 activity and impaired cycling (Kiyohara et al., 2006). We recently showed that this same region makes a significant contribution to binding both positive and negative transcriptional regulators by cooperating with a conserved alpha helical element in the TAD to influence clock timing (Xu et al., 2015). The data presented here identify yet another example of how the flexible BMAL1 TAD influences circadian timing and demonstrate the functional importance of protein dynamics at the TAD over an apparent twelve orders of magnitude.

Proline isomerization has demonstrated roles at each step of transcriptional regulation, from protein folding and regulation of transcription factor interactions, to modification and recognition of histone tails, and conformational control of the RNA Pol II C-terminal domain that controls its activity (reviewed in (Hanes, 2015)). Although we provide evidence in support of a binary conformational switch in the TAD by NMR and its ability to influence circadian timekeeping in cellular reconstitution assays, we still don't understand exactly how the switch regulates circadian period. Timekeeping by the circadian clock depends on the regulated transition through a series of transcriptional regulatory complexes on DNA throughout the day (Koike et al., 2012). This dynamic conformational switch could hinder the formation of highly stable complexes to play a role in the recognition and handoff between transcriptional coactivators and repressors at CLOCK:BMAL1. Other transcription factors such as p53, c-Myb and CREB utilize conformational changes at their TADs to control their activation state. While this most commonly arises from binding-induced changes in structure (Borcherds et al., 2014; Parker et al., 1999; Sugase et al., 2007), there is also evidence that slow events controlled by proline isomerization can play an important role in some cases (Follis et al., 2015). Our data demonstrate that both W624 and P625 establish the switch and contribute to normal circadian timekeeping. Interestingly, the W624A mutation not only locks the switch into its *trans* isomer, but also leads to an additional shortening of the period that is strikingly similar to the phenotype observed upon deletion of the entire switch region (Xu et al., 2015). Therefore, we believe that identifying the structural role that W624 plays in assembling complexes with transcriptional regulators will likely help identify how the TAD switch regulates CLOCK:BMAL1 activity.

Author Manuscript Author Manuscript Author Manuscript Author Manuscript

To date, conformational control by proline isomerization has been relatively poorly studied due to the difficulty in identification and analysis of the process *in vitro* and in the cellular milieu. Similarly, our understanding of the peptidyl-prolyl isomerases that regulate this intrinsically slow process in the cellular context has lagged behind that of other signaling enzymes like kinases and phosphatases. We have a solid understanding how kinases, phosphatases and other enzymes that control chemical modification of clock proteins exert powerful roles in modulating clock timing (Gallego and Virshup, 2007). We provide evidence here that isomerases of the cyclophilin family accelerate the intrinsically slow *cis*/*trans* isomerization of the BMAL1 TAD by up to several hundred-fold *in vitro*. Moreover, studies with the broad specificity inhibitor CsA suggest that cyclophilins contribute to circadian timekeeping in cells in a TAD switch-dependent manner. Interestingly, we found that a number of cyclophilins that are active on the BMAL1 TAD are also expressed *in vivo* on a circadian timescale, suggesting the possibility for modes of feedback regulation that are common in circadian rhythms (Baggs et al., 2009). These findings are strengthened by the observation that animals with chronic administration of peptidyl-prolyl isomerases inhibitors exhibit defects in circadian cycling (Katz et al., 2008), as do organ transplant patients on long-term dosing of CsA (Kooman et al., 2001; van de Borne et al., 1993; van den Dorpel et al., 1996). More work is needed to parse out the potentially redundant roles of cyclophilins and possibly other proline isomerases on the BMAL1 TAD. However, our findings are consistent with two studies showing that the isomerase PPIE (also known as Cyp33) binds to the histone methyltransferase MLL1 to modulate its activity (Wang et al., 2010), which is in turn recruited to the CLOCK:BMAL1 complex in a circadian-dependent manner (Katada and Sassone-Corsi, 2010). Conceivably, MLL1-bound PPIE may also promote prolyl isomerization within the BMAL1 TAD when assembled within a CLOCK:BMAL1:MLL1 complex, lending credence to a model that these ubiquitous enzymes may be recruited to and act upon the molecular timer in a circadian fashion.

STAR Methods

CONTACT FOR REAGENTS AND RESOURCE SHARING

Further information and requests for resources and reagents should be directed to and will be fulfilled by the Lead Contact, Carrie Partch (cpartch@ucsc.edu).

EXPERIMENTAL MODEL AND SUBJECT DETAILS

Cell lines—Isolated of the *Bmal1*$^{-/-}$; *Per2*^{Luc} line was previously described (Liu et al., 2008). The U2OS *Bmal1-dLuc* cell line was a gift from John Hogenesch (University of Cincinnati). Both cell lines were cultured in 10% DMEM (i.e. 10% (vol/vol) FBS) and 1X penicillin-streptomycin (Thermo Fisher) at 37°C in an incubator humidified with 5% CO_2. Cell lines were not authenticated.

METHOD DETAILS

Lentiviral DNA constructs, transduction, and analysis—Flag-tagged mouse *Bmal1* was cloned into pENTR/D-TOPO vector (Life Technologies) then recombined with pLV7 destination vector as previously described (Ramanathan et al., 2012). Mutations were introduced by PCR-based mutagenesis and all constructs were verified by sequencing.

Author Manuscript Author Manuscript Author Manuscript Author Manuscript

Production of recombinant lentiviral particles, infection and selection of *Bmal1*-complemented *Bmal1*$^{-/-}$; *Per2*^{Luc} lines was performed as described previously (Liu et al., 2008). Clonal cell lines were validated by genomic sequencing of the complemented *Bmal1* gene.

Expression of Flag-tagged *Bmal1* genes in the complemented cell lines was analyzed as before (Xu et al., 2015). Briefly, cells were lysed in RIPA buffer containing complete protease and phosphatase inhibitors (Sigma). Immunoblotting was done using the following primary antibodies: mouse anti-Flag (M2) (Sigma Cat. # F3165) and goat anti-beta actin (C-11) (Santa Cruz Biotechnology Cat. # sc-1615), and the following secondary antibodies: anti-mouse IgG-HRP (Santa Cruz Biotechnology Cat. # sc-2005) and anti-goat IgG-HRP (Santa Cruz Biotechnology Cat. # sc-2020). SuperSignal West Pico substrate (Pierce) was used for chemiluminescent detection on autoradiograph film.

Bioluminescence recording and data analysis—For real-time recording of bioluminescence, *Bmal1*$^{-/-}$; *Per2*^{Luc} and U2OS *Bmal1-dLuc* cell lines were grown to confluence in 35 mm dishes in 10% DMEM at 37°C in an incubator humidified with 5% CO_2. All cell lines were synchronized with addition of 100 nM dexamethasone in recording medium, which contained phenol red-free DMEM with 25 mM HEPES, pH 7.4, 1% (vol/vol) FBS, 1 mM luciferin and a 1X B-27 vitamin supplement (Thermo Fisher Cat. #17504044). Dishes were sealed using vacuum grease with a round 40 mm glass coverslip to minimize evaporation, and then moved to a 37°C incubator (without humidification) containing a LumiCycle luminometer. For experiments with inhibitors, lyophilized stocks of Cyclosporin A (Sigma cat. # 30024) and Deltamethrin (Sigma cat. #D9315) were resuspended in sterile DMSO. Stocks were further diluted in DMSO such that addition of the same volume of inhibitors resulted in a final concentration of DMSO of 0.3% (vol/vol) in culture. Inhibitor stocks were pipetted into recording medium, evenly mixed, and then added to cells.

A LumiCycle luminometer (Actimetrics) was used to monitor the luminescence (counts/sec) as a function of time and data were analyzed using the LumiCycle Analysis program (version 2.54, Actimetrics). The first 24 hours of recording were omitted from data processing, and then the raw data were baseline corrected and fit to a damped sine wave, from which period length, goodness of fit, amplitude and damping rate were determined. Data were deemed acceptable if the goodness of fit exceeded 80%. For *Bmal1*$^{-/-}$; *Per2*^{Luc} cells, at least two dishes per clonal line were tested for each run with four repeats (n = 8–12). The mean trace of all recordings with standard deviation is reported.

Expression and purification of recombinant proteins—Mouse BMAL1 TAD (residues 579–626) was cloned into a bacterial expression plasmid based on the pET22b vector backbone from the parallel vector series (Sheffield et al., 1999). The BMAL1 short TAD (residues 594–626) was codon optimized for expression in *E. coli* (GeneWiz) and cloned into the same vector. All constructs possessed an N-terminal TEV cleavable His_6GST solubilizing tag and ampicillin resistance. Mutations were introduced in the TAD using a modified protocol for site-directed mutagenesis (Liu and Naismith, 2008) and confirmed with sequencing. The bacterial expression plasmid encoding the mouse CBP KIX domain

Author Manuscript Author Manuscript Author Manuscript Author Manuscript

(residues 585–672) was a gift from Peter Wright (The Scripps Research Institute). CBP KIX has native histidine residues that allow for the purification of the protein using Ni-NTA resin.

The Rosetta (DE3) strain of *E. coli* containing plasmids with either BMAL1 TAD or CBP KIX were grown to an OD_{600} of ~0.6–0.9 in the presence of ampicillin (100 μg/mL) and chloramphenicol (35 μg/mL). Protein expression was induced with 0.5 mM isopropyl β-D-1-thiogalactopyranoside (IPTG) and allowed to proceed for 16–18 hours at 18°C in eithe r Luria Broth (LB) or M9 minimal medium containing 1g/L $^{15}NH_4Cl$ to generate uniformly ^{15}N-labeled proteins for NMR spectroscopy. Cells were lysed in with an Emulsiflex C-3 cell disruptor (Avestin) in Buffer A containing 50 mM Tris pH 7.5, 300 mM NaCl and 20 mM imidazole. The soluble fraction of *E. coli* lysates was passed over Ni-NTA resin (QIAGEN), washed thoroughly, and eluted using 250 mM imidazole. Fractions of interest were buffer exchanged into lysis buffer using a stirred-cell pressure concentrator with 3 kDa molecular weight cutoff filters (Amicon). Proteolysis was performed with His_6-tagged TEV protease overnight at 4°C and cleaved protein was retained from the flow-through of a Ni-NTA column. The purified protein was further purified on a preparative grade Superdex 75 16/600 size-exclusion column (GE Life Sciences) pre-equilibrated with NMR buffer (10 mM MES, pH 6.5 and 50 mM NaCl).

All of the bacterial expression constructs for human cyclophilins were previously described (Davis et al., 2010). Where possible, full-length proteins were expressed. However, isolated isomerase domains were expressed from the large, multidomain cyclophilins PPWD, PPIG, CWC27 due to solubility issues expressing full-length proteins. PPIH, PPIL3 and PPIG were cloned into the pET22b-based parallel vector system (Sheffield et al., 1999) with TEV-cleavable tags; PPIH and PPIL3 had a His_6GST tag to enhance yield and stability, and PPIG had a His_6 tag.

Rosetta (DE3) cells containing cyclophilin expression plasmids were grown at 37°C in LB with appropriate antibiotics until they reached OD_{600} 0.8–1. Expression was induced with 0.5 mM IPTG and then the growth was continued overnight at 16°C. Cells were resuspended in Buffer A, lysed in a cell disruptor, and then purified by Ni-NTA column according to manufacturer's protocol (QIAGEN). Tags were not cleaved with the exception of His_6GST-PPIH, which was subjected to overnight incubation with His_6-TEV protease at 4°C. The cleaved His 6GST tag was removed by passing the sample over Ni/NTA resin. All cyclophilins were further purified by running on a preparative grade Superdex 75 16/600 size-exclusion column pre-equilibrated with 20 mM HEPES pH 7.0, 100 mM NaCl, and 2 mM TCEP. For His_6GST-PPIL3, the fusion protein tag was not cleaved and the pH was increased to pH 7.5 to increase stability of the purified protein at room temperature.

Using the baculovirus expression system (Invitrogen), the His_6-tagged photolyase homology region (PHR, residues 1–491) of mouse CRY1 was expressed in Sf9 suspension insect cells (Expression Systems). Cells were infected with a high titer P3 virus at 1.5×10^6 cells/mL and grown for 72 hours with gentle shaking at 27°C. Following brief centr ifugation at 4,000 rpm, cells were resuspended in 50 mM Tris pH 7.5, 200 mM NaCl, 20 mM imidazole, 10% (vol/vol) glycerol, 0.2% (vol/vol) Triton X-100, 0.1% (vol/vol) NP40, 0.4% (vol/vol)

Author Manuscript Author Manuscript Author Manuscript Author Manuscript

Tween-20, 5 mM β-mercaptoethanol and 1X EDTA-free protease inhibitors (Pierce). Cells were lysed using a cell disruptor followed by brief sonication on ice with a ¼" probe (3 pulses of 15 sec. on/30 sec. off). Lysate was clarified by centrifugation at 37,000 rpm at 4°C for 1 hour. His_6-CRY1 protein was isolated by Ni-NTA agarose affinity chromatography, and then further purified by size-exclusion chromatography on a preparative grade Superdex 200 16/600 column (GE Life Sciences) pre-equilibrated with 20 mM HEPES pH 7.5, 125 mM NaCl, 5% (vol/vol) glycerol and 2 mM TCEP. Prior to fluorescence anisotropy experiments, all purified proteins were buffer exchanged into assay buffer: 50 mM Bis-Tris Propane, 100 mM NaCl, 2 mM TCEP and 0.05% (vol/vol) Tween-20.

Peptide synthesis and purification—8-mer switch peptides DFSDLPWPL, FSDLPWPL, FSDLPAPL, FSDLPWAL were synthesized by solid phase peptide synthesis on 3-chlortrityl resin with standard Fmoc chemistry. One or two 1:4:4:4:6 molar ratio of resin:HBTU:HOAT:Fmoc-AA-OH:DiPEA coupling reactions were performed in DMF for each amino acid addition. The *cis*-locked peptide FSDLPWdmPL (dmP, 5,5-dimethyl L-proline) was synthesized by solid phase peptide synthesis using standard Fmoc chemistry. Coupling of dmP onto the Leu-Resin was performed using 1:2:2:4 molar ratio of Resin:HATU:Fmoc-dmP-OH:DiPEA, and coupling of the Trp onto the Resin-Leu-dmP was performed using 1:3.8:4:6 molar ratio of Rsin:COMU:Fmoc-Trp-Boc-OH:DiPEA; all other coupling reactions were performed using HBTU/HOAT as described above. Naturally occurring Fmoc-protected amino acids were purchased from Fluka, Nova Biochem, AAPPTec, or Sigma Aldrich. Fmoc-dmP was purchased from PolyPeptide Group (Cat. # FA21702). Peptides were purified by reverse phase C18 HPLC; purity (>90%) and identity were verified by MS/MS on a Waters HPLC-MS/MS system.

The BMAL1 short TAD (residues 594–626) containing the P625dmP mutation and 8-mer switch peptides FSDLPFPL, FSDLPYPL and the insect BMAL1 peptide FSGLPWPLP were purchased from Bio-Synthesis Inc. The mouse CRY1 CC peptide (residues 471–503) was synthesized and purified as described previously (Xu et al., 2015).

Mass spectrometry—The ^{15}N BMAL1 TAD NMR sample was separated by a Surveyor HPLC system (Thermo Finnegan) with the Proto 300 C4 reverse-phase column (Higgins Analytical, Inc) with 5 μm particle size. A 20 μL aliquot of the sample was injected at flow rate of 200 μL/min with an autosampler tray at a temperature setting of 4°C. The mobile phase consisted of solv ent A: 0.1% formic acid in HPLC-grade water and Solvent B: 0.1% formic acid in acetonitrile with the following gradient: time (t) =0 to 3 min 95% solvent A and 5% solvent B; t = 28 min, 35% A and 65% B; t = 28.01 to 30 min, 5% A and 95% B; T= 30.01 to 40 min, 95% A and 5% B. The sample was then analyzed using a linear ion trap LTQ mass spectrometer system (Thermo Finnegan). Proteins were detected by full scan MS mode (over the m/z 300–3000) in positive mode. The electrospray voltage was set to 5 kV. Mass measurements of deconvoluted ESI mass spectra of the reversed-phase peaks were generated by Magtran software (Zhang and Marshall, 1998).

NMR spectroscopy—NMR experiments were conducted on a Varian INOVA 600-MHz spectrometer equipped with ^{1}H, ^{13}C, ^{15}N triple resonance, Z-axis pulsed field gradient cryoprobe. Sample temperatures were calibrated with the use of an ethylene glycol standard

Author Manuscript Author Manuscript Author Manuscript Author Manuscript

supplied by Agilent. At each temperature, NMR samples were given a 30-minute equilibration time prior to calibration and data acquisition. All NMR data were processed using NMRPipe/NMRDraw (Delaglio et al., 1995). Chemical shift assignment of mBMAL1 TAD was previously reported (Xu et al., 2015). ^{15}N-^{1}H HSQC titrations of BMAL1 TAD were performed in a 300 μL volume of 100 μM ^{15}N BMAL1 TAD in NMR buffer (10 mM MES pH 6.5, 50 mM NaCl) with 10% (vol/vol) D_2O by stepwise addition of CBP KIX or CRY1 CC peptide, followed by concentration in an Amicon Ultra centrifugal filter with a 3 kDa molecular weight cutoff. All titration data were collected at 25°C. Titration data were analyzed with NMRViewJ (One Moon Scientific) using chemical shift perturbations defined by the equation $\Delta\delta_{TOT} = [(\Delta\delta^{1}H)^2 + (\chi(\Delta\delta^{15}N)^2]^{½}$ and normalized with the scaling factor $\chi = 0.5$ (Johnson, 2004).

^{15}N-^{1}H ZZ-exchange experiments (Farrow et al., 1994) were collected on 400 μM ^{15}N BMAL1 TAD in NMR buffer (10 mM MES pH 6.5, 50 mM NaCl) with 10% (vol/vol) D_2O with 24 interleaved mixing times ranging from 0–3 seconds (0, 0.05, 0.1, 0.25, 0.5, 0.75, 1,1.25, 1,5, 1.75, 2, 2.5, 3) at temperatures of 25, 35, 45, 55, 60 and 65°C. Integration of the auto and cross peak intensities for each mixing time were extracted using NMRViewJ (One Moon Scientific). Cross peak intensities were normalized to the nominal cross peak intensities at time t=0, and total intensity was set to the sum of the integrations of the *cis* and *trans* peaks at t=0. The exchange constant k_{ex} was calculated by fitting integration data to an exchange model for two-state interconversion as described by equations 1–4 (Kleckner and Foster, 2011; Palmer et al., 2001) using MATLAB (MathWorks).

$$I_{AA}(T)=\frac{1}{2}P_A\left[\left(\frac{(1-R^0{}_{1A}-R^0{}_{1B}+k_{ex}(\rho_B-\rho_A))}{\lambda_+-\lambda_-}\right)e^{-\lambda_- t}+(1+\left(\frac{(1-R^0{}_{1A}-R^0{}_{1B}+k_{ex}(\rho_B-\rho_A))}{\lambda_+-\lambda_-}\right)e^{-\lambda=t}\right] \quad (1)$$

$$I_{BB}(T)=\frac{1}{2}P_B\left[\left(\frac{(1-R^0{}_{1A}-R^0{}_{1B}+k_{ex}(\rho_B-\rho_A))}{\lambda_+-\lambda_-}\right)e^{-\lambda_- t}+(1+\left(\frac{(1-R^0{}_{1A}-R^0{}_{1B}+k_{ex}(\rho_B-\rho_A))}{\lambda_+-\lambda_-}\right)e^{-\lambda=t}\right] \quad (2)$$

$$I_{AB}(T)=P_B\left[\left(\frac{(k_{ex}P_A)}{\lambda_+-\lambda_-}\right)\left(e^{-\lambda_- t}-e^{-\lambda=t}\right)\right] \quad (3)$$

Author Manuscript Author Manuscript Author Manuscript Author Manuscript

$$I_{\mathrm{BA}}(T)=P_{\mathrm{BA}}\left[\left(\frac{(k_{\mathrm{ex}}P_{\mathrm{B}})}{\lambda_{+}-\lambda_{-}}\right)\left(e^{-\lambda_{-}t}-e^{-\lambda_{=}t}\right)\right] \quad (4)$$

I refers to the time dependence of the transfer amplitudes (represented by the build-up curves) for the *cis* (AA), *trans* (BB) and *trans* to *cis* (BA), and *cis* to *trans* (AB) interconversions. *P* refers to the population of the indicated state, k_{ex} is the stochastic exchange of molecules between the two states per second, t is time in seconds, T is temperature in Kelvin, and R1A and R1B are the longitudinal relaxation rate constants in the absence of exchange.

The interconversion rates of *cis* to *trans* (k_{-1}) and *trans* to *cis* (k_1) were calculated using the relative populations of the two isomers taken from the integrations using equations 5–7.

$$k_{\mathrm{ex}}=k_1+k_{-1} \quad (5)$$

$$k_1=k_{\mathrm{ex}}*P_{\mathrm{trans}} \quad (6)$$

$$k_{-1}=k_{\mathrm{ex}}*P_{\mathrm{cis}} \quad (7)$$

Rates of isomerization were extrapolated to 25°C and 37°C using the Eyring equation (equation 8). The free energy of isomerization was calculated based on transition state theory using equation 9 and the difference in free energy between the two isomers calculated using equation 10.

$$ln\frac{K}{T}=-\frac{\Delta H}{RT}+ln\frac{kB}{h}+\frac{\Delta S}{R} \quad (8)$$

$$\Delta G^{\neq}=-RTln\left(\frac{hK_{\mathrm{CT}}}{k_{\mathrm{B}}T}\right) \quad (9)$$

$$\Delta G=\left|\Delta G^{\neq}{}_{\mathrm{CT}}-\Delta G^{\neq}{}_{\mathrm{TC}}\right| \quad (10)$$

T is temperature, R is the gas constant, k_{B} is the Boltzmann constant, h is Planck's constant, and ΔH and ΔS are the activation enthalpy and entropy, respectively, of *cis* to *trans* (CT) and *trans* to *cis* (TC) isomerization. The free energy of the isomerization was calculated using equation 8.

Author Manuscript Author Manuscript Author Manuscript Author Manuscript

To assess rate enhancement of interconversion by cyclophilins, ^{15}N-^{1}H ZZ-exchange data were collected on 400 μM ^{15}N BMAL1 TAD with 100 μM cyclophilin (natural abundance) in cyclophilin NMR buffer, 20 mM HEPES pH 7.0, 100 mM NaCl, and 2 mM TCEP with 10% (vol/vol) D_2O. As described above, the pH of the buffer was increased to pH 7.5 for His_6GST-PPIL3 to increase stability of the purified protein at room temperature. ZZ data were collected as above, except that experiments were performed at room temperature (22.68°C). The fold enhancement of isomerization rates was determined by comparing the uncatalyzed rates with catalyzed rates extrapolated to room temperature for the isolated BMAL1 TAD.

Fluorescence anisotropy—The BMAL1 short TAD WT, P625A, P625dmP and Δswitch (594-F619Y) probes were purchased from Bio-Synthesis Inc. with a 5,6-TAMRA fluorescent probe covalently attached to the N-terminus. The C-terminus of the Δswitch peptide was amidated, while the others were left as a free carboxyl group to mimic the native C-terminal group of the TAD at L626. Equilibrium binding assays with CRY1 PHR were performed in 50 mM Bis-Tris Propane pH 7.5, 100 mM NaCl, 2 mM TCEP and 0.05% (vol/vol) Tween-20. With CBP KIX, the assay was performed in 10 mM MES, pH 6.5, 50 mM NaCl and 0.05% (vol/vol) Tween-20. Concentrated stocks of BMAL1 TAD probes were stored between 15–200 μM at −70°C and diluted into assay buffer to 50 nM alone and in the presence of increasing concentrations of test proteins. Plates were incubated at room temperature for 10–20 minutes prior to analysis. Binding was monitored by changes in fluorescence polarization with an EnVision 2103 multilabel plate reader (Perkin Elmer) with excitation at 531 nm and emission at 595 nm. The Hill coefficient (n_H) and equilibrium binding dissociation constant (K_D) were calculated by fitting the dose-dependent change in millipolarization (Δmp) to a one-site specific binding model in Prism 6.0 (GraphPad), with averaged Δmp values from duplicate or triplicate assays. Data shown are from a representative experiment (n=4 replicates) of three independent assays.

Isothermal titration calorimetry—ITC measurements were obtained as previously described (Xu et al., 2015). Briefly, proteins were extensively dialyzed at 4°C in 10 mM MES pH 6.5, 50 mM NaCl using a 2 kDa molecular cutoff filter dialysis tubing (Spectrum Labs) prior to collecting ITC data. ITC was performed on a MicroCal VP-ITC calorimeter at 25°C with a stir speed of 177 r.p.m., reference power of 10 μCal/sec and 10 μL injection sizes. Protein ratios for the cell and syringe for the ITC assays (3 independent runs for each complex) were 220–230 μM CBP KIX titrated into 20–25 μM BMAL1 TAD WT, P625A, or P625dmP (N = 0.6–0.9). All data were best fit by a one-site binding model using Origin software.

QUANTIFICATION AND STATISTICAL ANALYSIS

Where applicable, statistical parameters including sample size, precision measures (standard deviation, s.d.) and statistical significance are reported in the Figures and corresponding Figure Legends.

Cellular Period Analysis—A LumiCycle luminometer (Actimetrics) was used to monitor luminescence (in counts/sec) as a function of time, and data were analyzed using the

Author Manuscript Author Manuscript Author Manuscript Author Manuscript

LumiCycle Analysis program (version 2.54, Actimetrics). The first 24 hours of recording were omitted from data processing, and then the raw data were baseline corrected and fit to a damped sine wave, from which period length, goodness of fit, amplitude and damping rate were determined. Data were deemed acceptable if the goodness of fit exceeded 80%. For *Bmal1*$^{-/-}$; *Per2*^{Luc} cells, at least two dishes per clonal line were tested for each run with four repeats (n = 8–12). The mean trace of all recordings with s.d. is reported. Statistical significance between genotypes or drug treatments was assessed using an unpaired t test in Prism 6.0.

Analysis of *cis/trans* isomerization rates—Experimentally determined rate constants for isomerization were visualized on an Eyring plot with representative s.d. errors from the derivation of individual *cis-trans* and *trans-cis* exchange rates from the time series NMR data. Data points at 55°C, 60°C, and 65°C were fitted to a linear regression to extrapolate exchange rates, not fast enough to detect experimentally by NMR, at lower temperatures (e.g. 25°C and 37°C).

DATA AND SOFTWARE AVAILABILITY

Raw data from the following ^{15}N-^{1}H ZZ exchange NMR time series experiments on ^{15}N BMAL1 TAD is available at Mendeley Data:

- 25°C time series: doi:10.17632/4hs472w6wb.1
- 55°C time series: doi:10.17632/8yx9wzt9gh.1
- 60°C time series: doi:10.17632/gjfjvjpvdr.1
- 65°C time series: doi:10.17632/kn58vc7hww.1
- room temperature time series with PPIA: doi:10.17632/4txk4b3w5g.1
- room temperature time series with PPIE: doi:10.17632/pt8xjvjs2v.1
- room temperature time series with PPIF: doi:10.17632/x8yn6x28x8.1
- room temperature time series with PPIG: doi:10.17632/fh595ry88h.1
- room temperature time series with PPIH: doi:10.17632/mpykzm4kw2.1
- room temperature time series with PPIL1: doi:10.17632/f9fxfynfrb.1
- room temperature time series with PPIL2: doi:10.17632/cg8fb64p5f.1
- room temperature time series with PPIL3: doi:10.17632/fmhg69tcxf.1
- room temperature time series with PPWD: doi:10.17632/csc3c5hs32.1
- room temperature time series with CWC27: doi:10.17632/htvhkdt7rw.1

An algorithm for analysis of ZZ exchange NMR time series data (and instructions for its use in MATLAB) are available at Mendeley Data: doi:10.17632/w7ytgp2y9d.1.

Supplementary Material

Refer to Web version on PubMed Central for supplementary material.

Author Manuscript Author Manuscript Author Manuscript Author Manuscript

Acknowledgments

We thank John Hogenesch (University of Cincinnati) for the U2OS *Bmal1-dLuc* cell line and Peter Wright (The Scripps Research Institute) for a plasmid encoding the KIX domain of mouse CBP. Thanks to Joshua Schwochert, Cameron Pye and Scott Lokey for training and providing resources for custom peptide synthesis. We thank Walter Bray in the UCSC Chemical Screening Center and Qiangli Zhang in the UCSC Mass Spectrometry Facility for access to instrumentation. Funding for the UCSC Mass Spectrometry Facility provided by the W.M. Keck Foundation (grant 001768) and NIH National Center for Research Resources (S10RR020939). This work was supported by NIH grants R01 GM107069 (to C.L.P.) and R00 GM094293 (to T.L.D.), and NSF grant IOS-0920417 (to A.C.L.). A.K.M. was supported by NIH Ruth Kirschstein predoctoral fellowship F31 CA189660.

References

Adams BM, Coates MN, Jackson SR, Jurica MS, Davis TL. Nuclear cyclophilins affect spliceosome assembly and function in vitro. Biochem J. 2015; 469:223–233. [PubMed: 25967372]

Baggs JE, Price TS, DiTacchio L, Panda S, Fitzgerald GA, Hogenesch JB. Network features of the mammalian circadian clock. PLoS biology. 2009; 7:e52. [PubMed: 19278294]

Bataille AR, Jeronimo C, Jacques PE, Laramee L, Fortin ME, Forest A, Bergeron M, Hanes SD, Robert F. A universal RNA polymerase II CTD cycle is orchestrated by complex interplays between kinase, phosphatase, and isomerase enzymes along genes. Molecular cell. 2012; 45:158–170. [PubMed: 22284676]

Borcherds W, Theillet FX, Katzer A, Finzel A, Mishall KM, Powell AT, Wu H, Manieri W, Dieterich C, Selenko P, et al. Disorder and residual helicity alter p53-Mdm2 binding affinity and signaling in cells. Nat Chem Biol. 2014; 10:1000–1002. [PubMed: 25362358]

Brazin KN, Mallis RJ, Fulton DB, Andreotti AH. Regulation of the tyrosine kinase Itk by the peptidyl-prolyl isomerase cyclophilin A. Proceedings of the National Academy of Sciences of the United States of America. 2002; 99:1899–1904. [PubMed: 11830645]

Chang DC, McWatters HG, Williams JA, Gotter AL, Levine JD, Reppert SM. Constructing a feedback loop with circadian clock molecules from the silkmoth, Antheraea pernyi. The Journal of biological chemistry. 2003; 278:38149–38158. [PubMed: 12869551]

Coelmont L, Hanoulle X, Chatterji U, Berger C, Snoeck J, Bobardt M, Lim P, Vliegen I, Paeshuyse J, Vuagniaux G, et al. DEB025 (Alisporivir) inhibits hepatitis C virus replication by preventing a cyclophilin A induced cis-trans isomerisation in domain II of NS5A. PloS one. 2010; 5:e13687. [PubMed: 21060866]

Czarna A, Berndt A, Singh HR, Grudziecki A, Ladurner AG, Timinszky G, Kramer A, Wolf E. Structures of Drosophila cryptochrome and mouse cryptochrome1 provide insight into circadian function. Cell. 2013; 153:1394–1405. [PubMed: 23746849]

Davis TL, Walker JR, Campagna-Slater V, Finerty PJ, Paramanathan R, Bernstein G, MacKenzie F, Tempel W, Ouyang H, Lee WH, et al. Structural and biochemical characterization of the human cyclophilin family of peptidyl-prolyl isomerases. PLoS biology. 2010; 8:e1000439. [PubMed: 20676357]

Delaglio F, Grzesiek S, Vuister GW, Zhu G, Pfeifer J, Bax A. NMRPipe: a multidimensional spectral processing system based on UNIX pipes. Journal of biomolecular NMR. 1995; 6:277–293. [PubMed: 8520220]

Eckert B, Martin A, Balbach J, Schmid FX. Prolyl isomerization as a molecular timer in phage infection. Nat Struct Mol Biol. 2005; 12:619–623. [PubMed: 15937494]

Enan E, Matsumura F. Specific inhibition of calcineurin by type II synthetic pyrethroid insecticides. Biochem Pharmacol. 1992; 43:1777–1784. [PubMed: 1315545]

Farrow NA, Zhang O, Forman-Kay JD, Kay LE. A heteronuclear correlation experiment for simultaneous determination of 15N longitudinal decay and chemical exchange rates of systems in slow equilibrium. Journal of biomolecular NMR. 1994; 4:727–734. [PubMed: 7919956]

Ferrell JE Jr, Cimprich KA. Enforced proximity in the function of a famous scaffold. Molecular cell. 2003; 11:289–291. [PubMed: 12620218]

Author Manuscript Author Manuscript Author Manuscript Author Manuscript

Follis AV, Llambi F, Merritt P, Chipuk JE, Green DR, Kriwacki RW. Pin1-Induced Proline Isomerization in Cytosolic p53 Mediates BAX Activation and Apoptosis. Molecular cell. 2015; 59:677–684. [PubMed: 26236013]

Gallego M, Virshup DM. Post-translational modifications regulate the ticking of the circadian clock. Nature reviews. Molecular cell biology. 2007; 8:139–148. [PubMed: 17245414]

Grathwohl C, Wuthrich K. NMR studies of the rates of proline cis-trans isomerization in oligopeptides. Biopolymers. 1981; 15:2623–2633.

Gustafson CL, Partch CL. Emerging models for the molecular basis of Mammalian circadian timing. Biochemistry. 2015; 54:134–149. [PubMed: 25303119]

Hanes SD. Prolyl isomerases in gene transcription. Biochimica et biophysica acta. 2015; 1850:2017–2034. [PubMed: 25450176]

Henzler-Wildman K, Kern D. Dynamic personalities of proteins. Nature. 2007; 450:964–972. [PubMed: 18075575]

Huai Q, Kim HY, Liu Y, Zhao Y, Mondragon A, Liu JO, Ke H. Crystal structure of calcineurin-cyclophilin-cyclosporin shows common but distinct recognition of immunophilin-drug complexes. Proceedings of the National Academy of Sciences of the United States of America. 2002; 99:12037–12042. [PubMed: 12218175]

Hughes ME, DiTacchio L, Hayes KR, Vollmers C, Pulivarthy S, Baggs JE, Panda S, Hogenesch JB. Harmonics of circadian gene transcription in mammals. PLoS genetics. 2009; 5:e1000442. [PubMed: 19343201]

Hughes ME, Hogenesch JB, Kornacker K. JTK_CYCLE: an efficient nonparametric algorithm for detecting rhythmic components in genome-scale data sets. Journal of biological rhythms. 2010; 25:372–380. [PubMed: 20876817]

Johnson BA. Using NMRView to visualize and analyze the NMR spectra of macromolecules. Methods Mol Biol. 2004; 278:313–352. [PubMed: 15318002]

Kang SW, Lee E, Cho E, Seo JH, Ko HW, Kim EY. Drosophila peptidyl-prolyl isomerase Pin1 modulates circadian rhythms via regulating levels of PERIOD. Biochemical and biophysical research communications. 2015; 463:235–240. [PubMed: 25998391]

Katz ME, Simonetta SH, Ralph MR, Golombek DA. Immunosuppressant calcineurin inhibitors phase shift circadian rhythms and inhibit circadian responses to light. Pharmacol Biochem Behav. 2008; 90:763–768. [PubMed: 18590756]

Kiyohara YB, Tagao S, Tamanini F, Morita A, Sugisawa Y, Yasuda M, Yamanaka I, Ueda HR, van der Horst GT, Kondo T, et al. The BMAL1 C terminus regulates the circadian transcription feedback loop. Proceedings of the National Academy of Sciences of the United States of America. 2006; 103:10074–10079. [PubMed: 16777965]

Kleckner IR, Foster MP. An introduction to NMR-based approaches for measuring protein dynamics. Biochimica et biophysica acta. 2011; 1814:942–968. [PubMed: 21059410]

Koike N, Yoo SH, Huang HC, Kumar V, Lee C, Kim TK, Takahashi JS. Transcriptional architecture and chromatin landscape of the core circadian clock in mammals. Science. 2012; 338:349–354. [PubMed: 22936566]

Kooman JP, Christiaans MH, Boots JM, van Der Sande FM, Leunissen KM, van Hooff JP. A comparison between office and ambulatory blood pressure measurements in renal transplant patients with chronic transplant nephropathy. Am J Kidney Dis. 2001; 37:1170–1176. [PubMed: 11382685]

Lang K, Schmid FX, Fischer G. Catalysis of protein folding by prolyl isomerase. Nature. 1987; 329:268–270. [PubMed: 3306408]

Lee C, Etchegaray JP, Cagampang FR, Loudon AS, Reppert SM. Posttranslational mechanisms regulate the mammalian circadian clock. Cell. 2001; 107:855–867. [PubMed: 11779462]

Lin DT, Lechleiter JD. Mitochondrial targeted cyclophilin D protects cells from cell death by peptidyl prolyl isomerization. The Journal of biological chemistry. 2002; 277:31134–31141. [PubMed: 12077116]

Liou YC, Zhou XZ, Lu KP. Prolyl isomerase Pin1 as a molecular switch to determine the fate of phosphoproteins. Trends Biochem Sci. 2011; 36:501–514. [PubMed: 21852138]

Author Manuscript Author Manuscript Author Manuscript Author Manuscript

Lipton JO, Yuan ED, Boyle LM, Ebrahimi-Fakhari D, Kwiatkowski E, Nathan A, Guttler T, Davis F, Asara JM, Sahin M. The Circadian Protein BMAL1 Regulates Translation in Response to S6K1-Mediated Phosphorylation. Cell. 2015; 161:1138–1151. [PubMed: 25981667]

Liu AC, Tran HG, Zhang EE, Priest AA, Welsh DK, Kay SA. Redundant function of REV-ERBalpha and beta and non-essential role for Bmal1 cycling in transcriptional regulation of intracellular circadian rhythms. PLoS genetics. 2008; 4:e1000023. [PubMed: 18454201]

Liu H, Naismith JH. An efficient one-step site-directed deletion, insertion, single and multiple-site plasmid mutagenesis protocol. BMC biotechnology. 2008; 8:91. [PubMed: 19055817]

Liu J, Farmer JD Jr, Lane WS, Friedman J, Weissman I, Schreiber SL. Calcineurin is a common target of cyclophilin-cyclosporin A and FKBP-FK506 complexes. Cell. 1991; 66:807–815. [PubMed: 1715244]

Lu KP, Finn G, Lee TH, Nicholson LK. Prolyl cis-trans isomerization as a molecular timer. Nat Chem Biol. 2007; 3:619–629. [PubMed: 17876319]

Lummis SC, Beene DL, Lee LW, Lester HA, Broadhurst RW, Dougherty DA. Cis-trans isomerization at a proline opens the pore of a neurotransmitter-gated ion channel. Nature. 2005; 438:248–252. [PubMed: 16281040]

Nakamura K, Greenwood A, Binder L, Bigio EH, Denial S, Nicholson L, Zhou XZ, Lu KP. Proline isomer-specific antibodies reveal the early pathogenic tau conformation in Alzheimer's disease. Cell. 2012; 149:232–244. [PubMed: 22464332]

Nelson CJ, Santos-Rosa H, Kouzarides T. Proline isomerization of histone H3 regulates lysine methylation and gene expression. Cell. 2006; 126:905–916. [PubMed: 16959570]

Pal D, Chakrabarti P. Cis peptide bonds in proteins: residues involved, their conformations, interactions and locations. Journal of molecular biology. 1999; 294:271–288. [PubMed: 10556045]

Palmer AG 3rd, Kroenke CD, Loria JP. Nuclear magnetic resonance methods for quantifying microsecond-to-millisecond motions in biological macromolecules. Methods Enzymol. 2001; 339:204–238. [PubMed: 11462813]

Park N, Kim HD, Cheon S, Row H, Lee J, Han DH, Cho S, Kim K. A Novel Bmal1 Mutant Mouse Reveals Essential Roles of the C-Terminal Domain on Circadian Rhythms. PloS one. 2015; 10:e0138661. [PubMed: 26394143]

Parker D, Rivera M, Zor T, Henrion-Caude A, Radhakrishnan I, Kumar A, Shapiro L, Wright P, Montminy M, Brindle P. Role of secondary structure in discrimination between constitutive and inducible activators. Molecular and cellular biology. 1999; 19:5601–5607. [PubMed: 10409749]

Partch CL, Green CB, Takahashi JS. Molecular architecture of the mammalian circadian clock. Trends Cell Biol. 2014; 24:90–99. [PubMed: 23916625]

Peterson KJ, Lyons JB, Nowak KS, Takacs CM, Wargo MJ, McPeek MA. Estimating metazoan divergence times with a molecular clock. Proceedings of the National Academy of Sciences of the United States of America. 2004; 101:6536–6541. [PubMed: 15084738]

Phillips AH, Zhang Y, Cunningham CN, Zhou L, Forrest WF, Liu PS, Steffek M, Lee J, Tam C, Helgason E, et al. Conformational dynamics control ubiquitin-deubiquitinase interactions and influence in vivo signaling. Proceedings of the National Academy of Sciences of the United States of America. 2013; 110:11379–11384. [PubMed: 23801757]

Pizarro A, Hayer K, Lahens NF, Hogenesch JB. CircaDB: a database of mammalian circadian gene expression profiles. Nucleic acids research. 2013; 41:D1009–1013. [PubMed: 23180795]

Pullen L, Bolon DN. Enforced N-domain proximity stimulates Hsp90 ATPase activity and is compatible with function in vivo. The Journal of biological chemistry. 2011; 286:11091–11098. [PubMed: 21278257]

Ramanathan C, Khan S, Kathale N, Xu H, Liu A. Monitoring cell-autonomous circadian clock rhythms of gene expression using luciferase bioluminescence reporters. Journal of visualized experiments: JoVE. 2012

Reimer U, Scherer G, Drewello M, Kruber S, Schutkowski M, Fischer G. Side-chain effects on peptidyl-prolyl cis/trans isomerisation. Journal of molecular biology. 1998; 279:449–460. [PubMed: 9642049]

Rubin EB, Shemesh Y, Cohen M, Elgavish S, Robertson HM, Bloch G. Molecular and phylogenetic analyses reveal mammalian-like clockwork in the honey bee (Apis mellifera) and shed new light

Author Manuscript Author Manuscript Author Manuscript Author Manuscript

on the molecular evolution of the circadian clock. Genome Res. 2006; 16:1352–1365. [PubMed: 17065608]

Saleh T, Jankowski W, Sriram G, Rossi P, Shah S, Lee KB, Cruz LA, Rodriguez AJ, Birge RB, Kalodimos CG. Cyclophilin A promotes cell migration via the Abl-Crk signaling pathway. Nat Chem Biol. 2016; 12:117–123. [PubMed: 26656091]

Sarkar P, Reichman C, Saleh T, Birge RB, Kalodimos CG. Proline cis-trans isomerization controls autoinhibition of a signaling protein. Molecular cell. 2007; 25:413–426. [PubMed: 17289588]

Schmid FX. Prolyl isomerase: enzymatic catalysis of slow protein-folding reactions. Annu Rev Biophys Biomol Struct. 1993; 22:123–142. [PubMed: 7688608]

Sheffield P, Garrard S, Derewenda Z. Overcoming expression and purification problems of RhoGDI using a family of “parallel” expression vectors. Protein Expr Purif. 1999; 15:34–39. [PubMed: 10024467]

Shen Y, Bax A. Prediction of Xaa-Pro peptide bond conformation from sequence and chemical shifts. Journal of biomolecular NMR. 2010; 46:199–204. [PubMed: 20041279]

Shi S, Hida A, McGuinness OP, Wasserman DH, Yamazaki S, Johnson CH. Circadian clock gene Bmal1 is not essential; functional replacement with its paralog, Bmal2. Current biology: CB. 2010; 20:316–321. [PubMed: 20153195]

Stewart DE, Sarkar A, Wampler JE. Occurrence and role of cis peptide bonds in protein structures. Journal of molecular biology. 1990; 214:253–260. [PubMed: 2370664]

Sugase K, Dyson H, Wright P. Mechanism of coupled folding and binding of an intrinsically disordered protein. Nature. 2007; 447:1021–1025. [PubMed: 17522630]

Theillet FX, Binolfi A, Frembgen-Kesner T, Hingorani K, Sarkar M, Kyne C, Li C, Crowley PB, Gierasch L, Pielak GJ, et al. Physicochemical properties of cells and their effects on intrinsically disordered proteins (IDPs). Chem Rev. 2014; 114:6661–6714. [PubMed: 24901537]

van de Borne P, Gelin M, Van de Stadt J, Degaute JP. Circadian rhythms of blood pressure after liver transplantation. Hypertension. 1993; 21:398–405. [PubMed: 8458641]

van den Dorpel MA, van den Meiracker AH, Lameris TW, Boomsma F, Levi M, Man in’t Veld AJ, Weimar W, Schalekamp MA. Cyclosporin A impairs the nocturnal blood pressure fall in renal transplant recipients. Hypertension. 1996; 28:304–307. [PubMed: 8707398]

Vollmers C, Panda S, DiTacchio L. A high-throughput assay for siRNA-based circadian screens in human U2OS cells. PloS one. 2008; 3:e3457. [PubMed: 18941634]

Wedemeyer WJ, Welker E, Scheraga HA. Proline cis-trans isomerization and protein folding. Biochemistry. 2002; 41:14637–14644. [PubMed: 12475212]

Xu H, Gustafson CL, Sammons PJ, Khan SK, Parsley NC, Ramanathan C, Lee HW, Liu AC, Partch CL. Cryptochrome 1 regulates the circadian clock through dynamic interactions with the BMAL1 C terminus. Nat Struct Mol Biol. 2015; 22:476–484. [PubMed: 25961797]

Zhang R, Lahens NF, Ballance HI, Hughes ME, Hogenesch JB. A circadian gene expression atlas in mammals: implications for biology and medicine. Proceedings of the National Academy of Sciences of the United States of America. 2014; 111:16219–16224. [PubMed: 25349387]

Zhang Z, Marshall AG. A universal algorithm for fast and automated charge state deconvolution of electrospray mass-to-charge ratio spectra. J Am Soc Mass Spectrom. 1998; 9:225–233. [PubMed: 9879360]

Zhou XZ, Lu KP. The isomerase PIN1 controls numerous cancer-driving pathways and is a unique drug target. Nature reviews. Cancer. 2016; 16:463–478.

Zhu H, Sauman I, Yuan Q, Casselman A, Emery-Le M, Emery P, Reppert SM. Cryptochromes define a novel circadian clock mechanism in monarch butterflies that may underlie sun compass navigation. PLoS biology. 2008; 6:e4.

Zondlo NJ. Aromatic-proline interactions: electronically tunable CH/pi interactions. Acc Chem Res. 2013; 46:1039–1049. [PubMed: 23148796]

Author Manuscript Author Manuscript Author Manuscript Author Manuscript

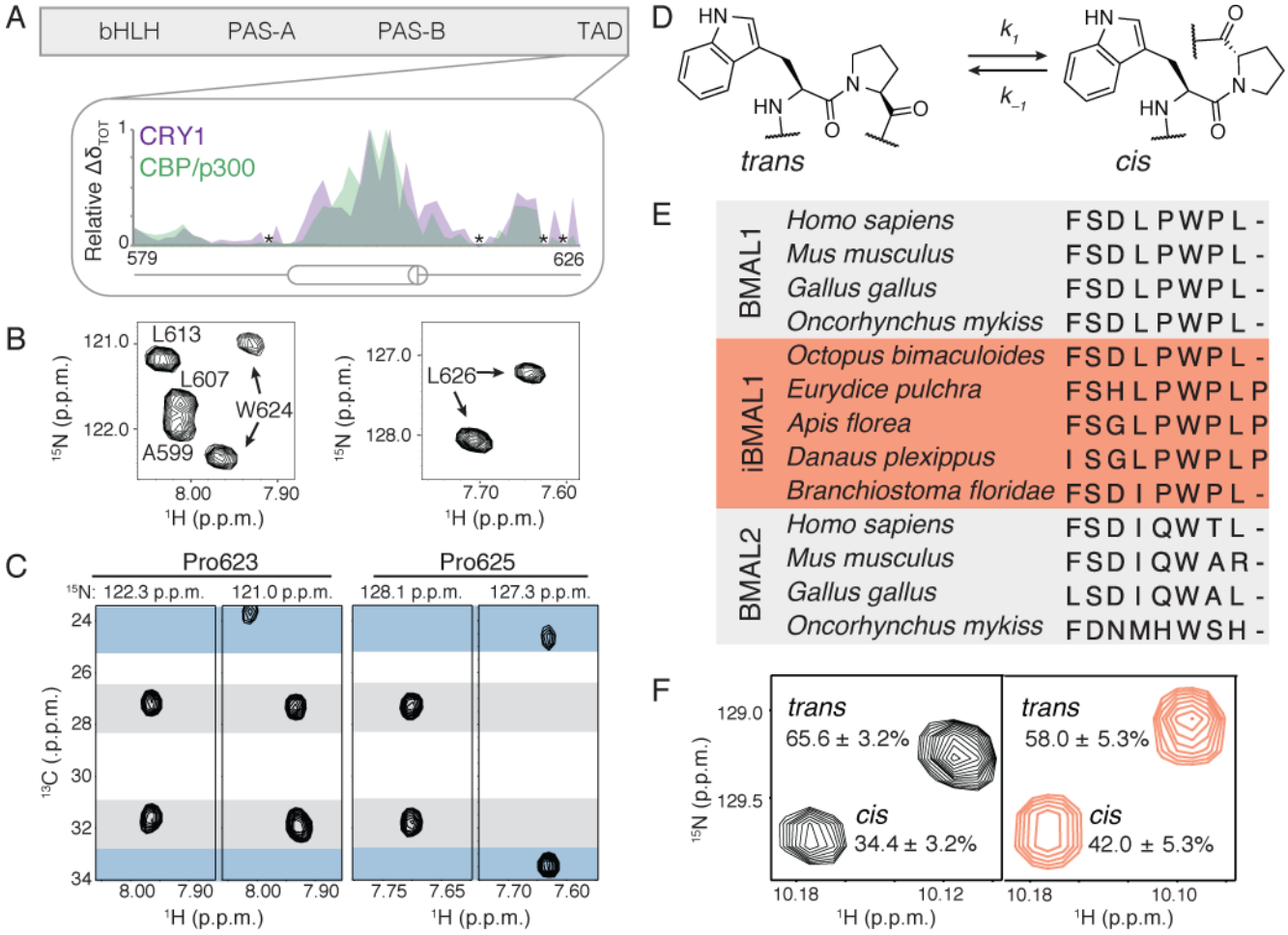

Figure 1. Isomerization about a conserved Trp-Pro imide bond in the BMAL1 C-terminal TAD

(A) Domain schematic of mouse BMAL1 showing the chemical shifts (Δδ) in the TAD after binding CRY1 CC helix (purple) or CBP KIX domain (green). *, proline residues that lack crosspeaks in ^{15}N-^{1}H HSQC NMR spectra. (B) Selected regions of ^{15}N-^{1}H HSQC spectra of ^{15}N BMAL1 TAD displaying backbone amide peaks for two isomers at W624 and L626. (C) Cross peaks for P623 and P625 C_β and C_γ atoms are shown in strips from the ^{15}N-edited (H)C(CO)NH-TOCSY of ^{13}C/^{15}N BMAL1 TAD at ^{15}N planes for W624 and L626 amides. Average ^{13}C shifts for *trans* (gray) and *cis* (blue) isomers from (Shen and Bax, 2010). (D) The W624-P625 imide bond in *cis* and *trans* conformations. (E) Sequence alignment BMAL1, BMAL2 and CYCLE from insects with a vertebrate-like clock (iBMAL1). (F) Regions of ^{15}N-^{1}H HSQC spectra of 8-mer switch peptides from mouse (FSDLPWPL, black) and dwarf honey bee (FSGLPWPLP, peach) showing *cis* and *trans* peaks for W624 indole. See also Figure S1.

Author Manuscript Author Manuscript Author Manuscript Author Manuscript

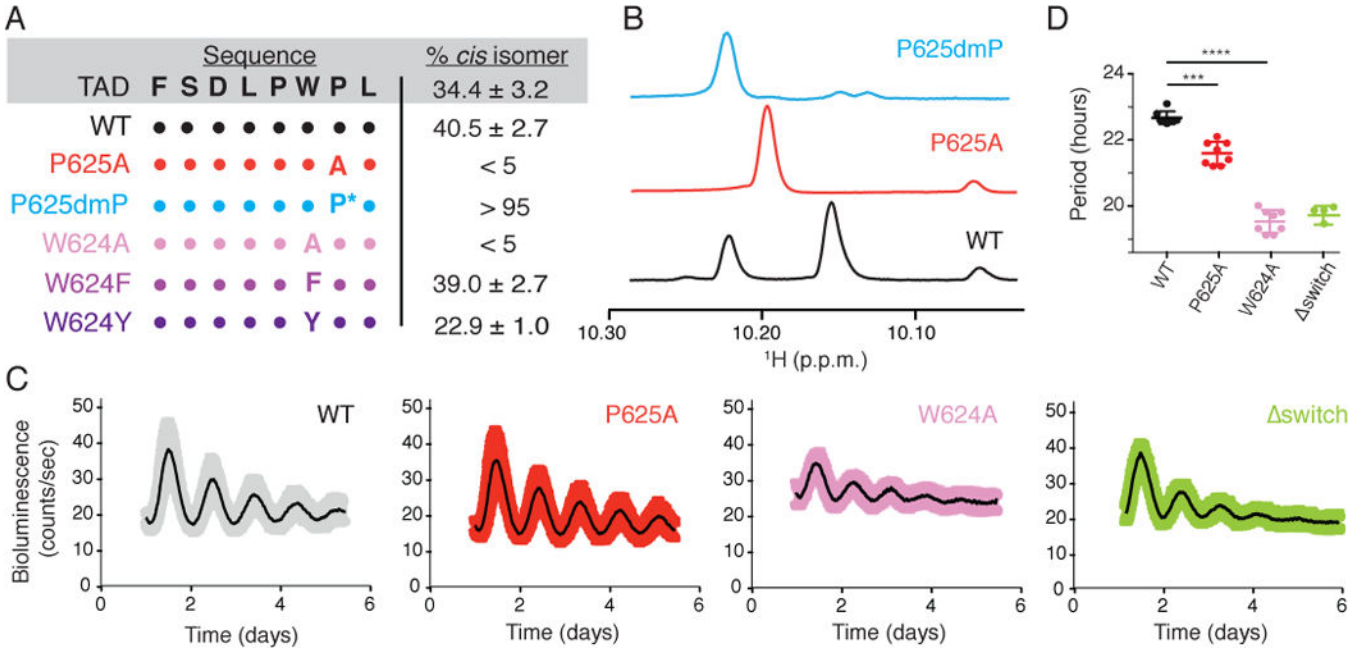

Figure 2. Locked mutants of the TAD switch shorten the circadian period

(A) Representation of *cis* content of 8-mer TAD switch peptides for P625 and W624 mutants compared to the intact ^{15}N BMAL1 TAD. *Cis* content was calculated from peak volumes of residues 624 and 626 in ^{15}N-^{1}H HSQC and ^{1}H-^{1}H TOCSY NMR spectra. (B) ^{1}H NMR spectra from FSDLPWPL (black), FSDLPWAL (red) and FSDLPWdmPL (blue) 8-mer TAD switch peptides highlighting the W624 indole region. (C) Synchronized circadian bioluminescence records from *Bmal1*$^{-/-}$; *Per2*^{Luc} mouse fibroblasts complemented with WT (gray), W624A (pink), P625A (red), or Δswitch (619X, green) *Bmal1*. Black line, mean luminescence ± s.d. from n = 6–8 replicates from 2 independent clonal lines in indicated colors. D) Circadian period of complemented fibroblast lines from panel (C). Individual period measurements with mean ± s.d. ***P<0.01 and ****P<0.0001 compared to WT *Bmal1* by two-tailed t test. See also Figure S2.

Author Manuscript Author Manuscript Author Manuscript Author Manuscript

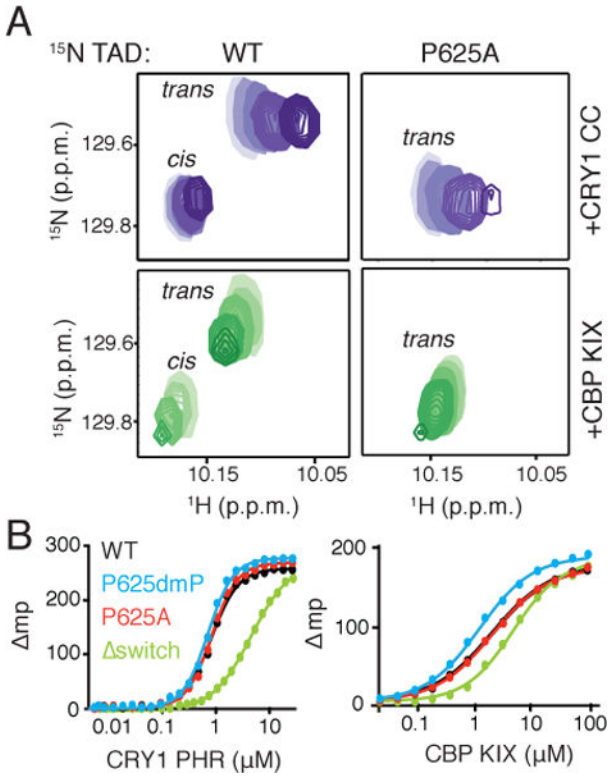

Figure 3. Both isomers of the TAD switch interact with transcriptional activators and repressors

(A) Regions of the ^{15}N-^{1}H HSQC spectra showing 100 μM WT (left panels) or P625A (right panels) ^{15}N BMAL1 TAD upon titration of CRY1 CC (purple) or CBP KIX (green), with increasing concentrations from 25–200 μM indicated by darker colors. (B) Fluorescence anisotropy data for CRY1 PHR (left) and CBP KIX (right) with wild type (black), P625A (red), P625dmP (blue) and Δswitch (green) 5,6-TAMRA-labeled short BMAL1 TAD (residues 594–626). Mean polarization data from one representative experiment (n = 4 replicates) of 3 independent assays. See also Figure S3.

Author Manuscript Author Manuscript Author Manuscript Author Manuscript

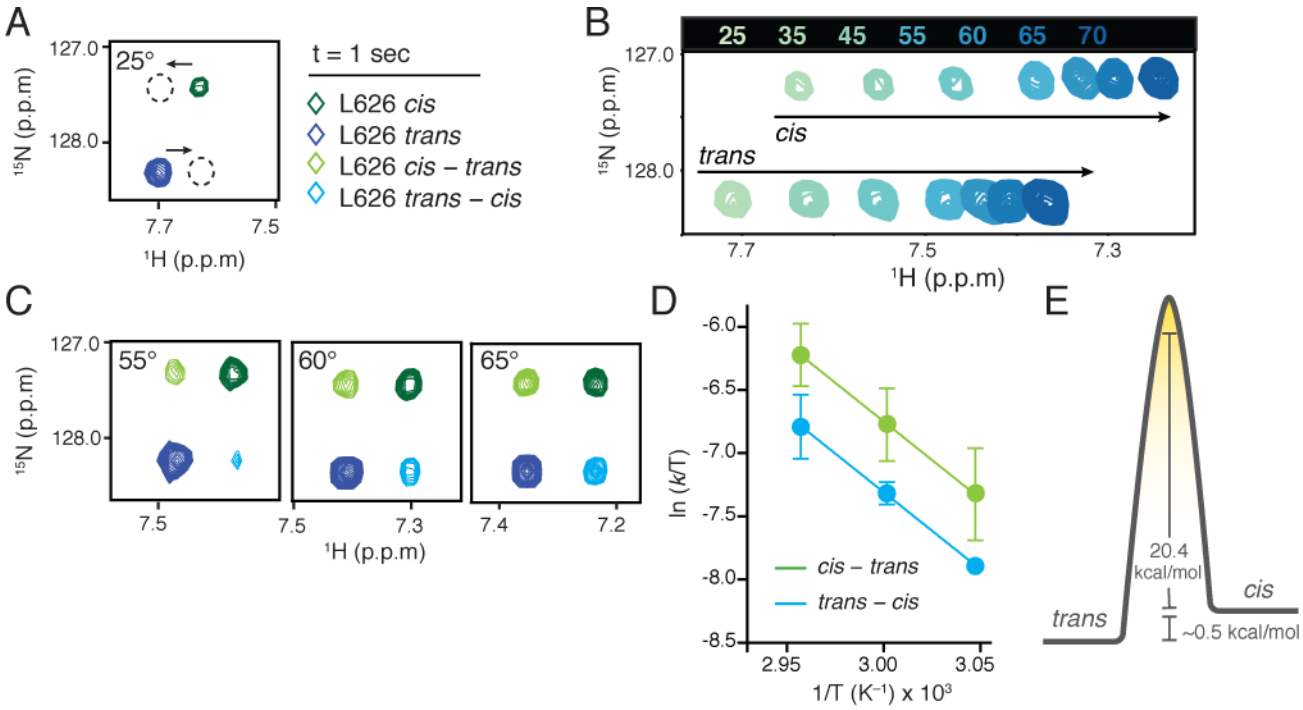

Figure 4. Slow isomerization of the TAD switch occurs on the timescale of minutes

(A) Highlighted region of the 2D spectrum from a ^{15}N-^{1}H ZZ-exchange assay performed at 25°C of ^{15}N BMAL1 TAD displaying *cis* (dark green), *trans* (dark blue), *cis* to *trans* (light green) and *trans* to *cis* (light blue) cross peaks for L626 at a delay = 1 s. Dashed circles, location of exchange cross peaks. (B) Overlay of ^{15}N-^{1}H HSQC spectra showing the *cis* and *trans* peaks of L626 at increasing temperatures. (C) Snapshot of ZZ-exchange assays at delay = 1 s at indicated temperatures. (D) Eyring analysis of exchange rates vs. temperature from ZZ-exchange assays with errors displayed in s.d. (E) Free energy plot showing the calculated activation energy of isomerization for the BMAL1 TAD. See also Figure S4.

Author Manuscript
Author Manuscript
Author Manuscript
Author Manuscript

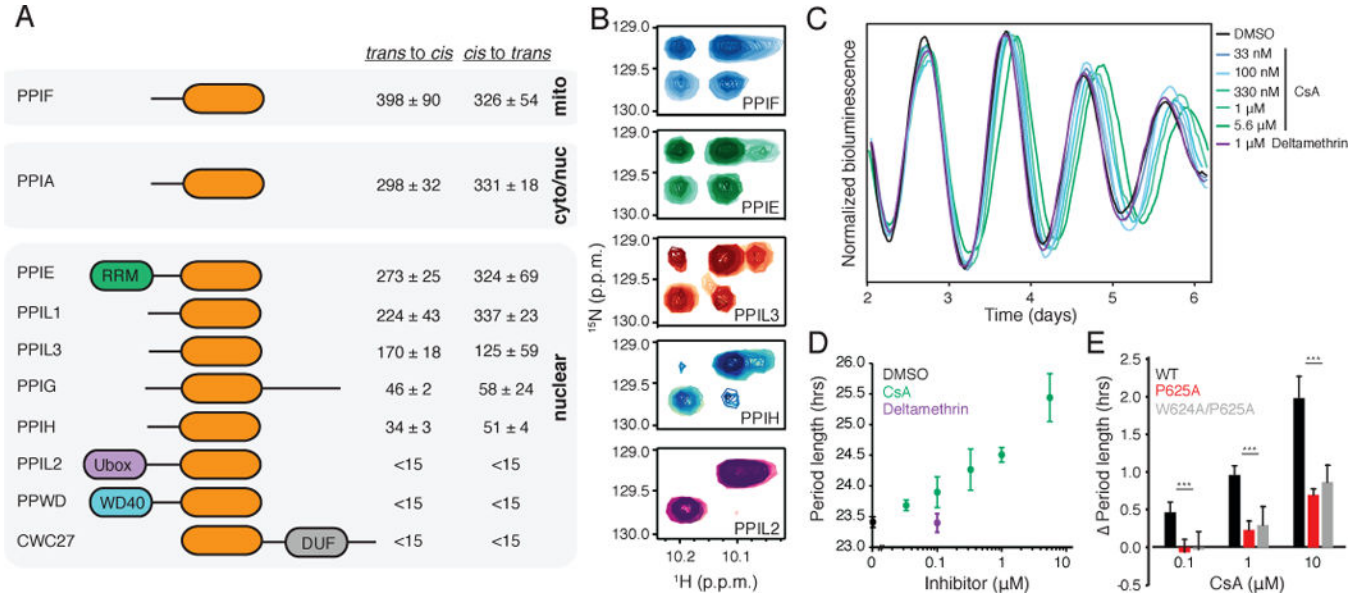

Figure 5. Cyclophilins accelerate isomerization of the TAD switch to regulate circadian period

(A) Domain schematics for cyclophilins tested against the BMAL1 TAD and relative rate enhancement compared to uncatalyzed isomerization at room temperature. (B) Highlighted region of ^{15}N-^{1}H ZZ-exchange spectra displaying the W624 indole of the ^{15}N TAD with indicated cyclophilins. Spectra from a ZZ-exchange time delay series (delay = 0–1 s) are overlaid in sequentially darker colors. (C) Synchronized circadian bioluminescence records from U2OS *Bmal1-dLuc* fibroblasts in the presence of DMSO, Cyclosporin A (CsA), or Deltamethrin. One individual trace shown for clarity from 2 independent assays with n = 3 replicates. (D) Mean circadian period of cultures upon treatment with DMSO (black), CsA (green) or Deltamethrin (purple) ± s.d. from n = 3 replicates with 2 independent assays. (E) Comparison of mean period changes ± s.d. as a function of CsA concentration in *Bmal1*$^{-/-}$; *Per2*^{Luc} fibroblasts complemented with WT (black), P625A (red), or W624A/P625A (gray) *Bmal1*. ***P<0.01 compared to WT *Bmal1* by two-tailed t test. See also Figure S5.

Author Manuscript

Author Manuscript

Author Manuscript

Author Manuscript

Table 1

Affinity of BMAL1 TAD mutants and conformationally-locked isomers for transcriptional regulators

	CRY1 PHR		CBP KIX	
BMAL1 TAD	**K_D (μM)**	**Hill**	**K_D (μM)**	**Hill**
Wild Type	0.90 ± 0.27	1.6 ± 0.1	1.34 ± 0.40	0.99 ± 0.13
P625A	0.99 ± 0.27	1.8 ± 0.1	1.59 ± 0.66	0.98 ± 0.28
P625dmP	0.86 ± 0.17	1.9 ± 0.1	1.16 ± 0.44	1.02 ± 0.48
Δswitch	4.28 ± 0.33	0.9 ± 0.04	4.63 ± 1.05	0.91 ± 0.19

Data were acquired by fluorescence polarization assay and fit to a one-site binding model with Prism 6.0. Values shown are averages of three or four independent experiments ± s.d. with n = 2 or 3 replicates each.

Author Manuscript

Author Manuscript

Author Manuscript

Author Manuscript

Table 2

Kinetics of *cis/trans* isomerization at the TAD switch as measured by ^{15}N-^{1}H ZZ-exchange NMR spectroscopy

	Rate of isomerization (s^{-1})		Time per isomerization event (s)	
Temperature (°C)	***cis*➔*trans***	***trans*➔*cis***	***cis*➔*trans***	***trans*➔*cis***
25*	4.58×10^{-3}	2.64×10^{-3}	218.34	378.78
37*	2.33×10^{-2}	1.35×10^{-2}	42.92	74.07
55	2.15×10^{-1}	1.24×10^{-1}	4.65	8.06
60	3.82×10^{-1}	2.20×10^{-1}	2.62	4.55
65	6.67×10^{-1}	3.84×10^{-1}	1.50	2.60

*Values extrapolated from Eyring plot